Analytical description of a plasma diffraction grating induced by two crossed laser beams

Luis Plaja and Luis Roso
Departamento de Física Aplicada, Universidad de Salamanca, E-37008 Salamanca, Spain
(Received 30 May 1997)

The possibility of inducing a gratinglike electronic distribution at the surface of a plasma irradiated by two crossed laser beams is analyzed for *s* and *p* beam polarizations. A simple relativistic model allows us to predict the fringe location, and to give an analytical expression for the time-averaged charge density. The stability of the grating structure depending on the beam polarization is also discussed. Finally, we test our conclusions in the light of the numerical integration of the Lorentz and Poisson equations by means of a one-dimensional particle-in-cell code. [S1063-651X(97)02412-4]

PACS number(s): 52.40.Nk, 52.65.Rr, 52.60.+h

I. INTRODUCTION

In the past decade, the availability of very intense sources of coherent electromagnetic radiation gave rise to a new field of study in optics: the interaction of matter with light well beyond the perturbative limit. Surprising new aspects rose in the field of atom-laser interactions, such as above-threshold ionization or the possibility of generating ultrahigh frequencies through harmonic generation [1].

The study of such nonperturbative phenomena beyond the single-atom approximation is a more recent concern, since it involves a more complicated theoretical treatment. A typical scenario for these multiparticle approaches is the interaction of intense laser beams with solids. In fact, we witnessed increasing activity in this field in the past few years. Although some work carried on in the description of nonresonant interaction with the bulk of semiconductor materials [2], the increase of the intensity of the laser sources leads to situations in which complete ionization at the material surface is achieved after a few cycles. Surface plasma dynamics becomes, therefore, a major source of nonlinearities, especially when the density exceeds the critical value [3]. For this case, experiments [4,5] and theory [6,7] show the presence of high-order harmonics in the reflected light. Particle-in-cell (PIC) calculations [8] are widely used in theoretical descriptions of such phenomena, although simpler moving mirror models [6,9,10] give a reasonable description. On the other hand, properties of laser-induced gratings were intensively studied in the 1980s [11]. Bragg diffraction and forward-stimulated Brillouin scattering on a configuration similar to the one presented here have been also studied [12].

One possible application of field-induced plasma diffraction gratings is in the interaction of high-intensity fields with solid surfaces. The intense fields generated by chirped pulse amplification techniques were prevented from reaching the target surface by the plasma already generated in the prepulse. In the case of an induced diffraction grating, when the plasma density is close to the critical density, underdense grating fringes are alternated spatially with overdense ones. If the grating structure is induced at the prepulse stage, the underdense regions will allow for deeper field penetration when the main pulse arrives.

In this paper we test the possibility of generating plasma surface-grating structures under high-intensity radiation. We will show that they are stable in the *s*-polarization laser configuration, while unstable in the *p*-polarization case. PIC simulations will be presented in support. Finally, we derive analytical expressions that approximate the averaged electron density for the *s*-polarization case, and enclose information of the fringe parameters (maximum electron density and fringe width), valid widely except in the far ultrarelativistic regime. According to the above paragraph, we will restrict ourselves to the case in which the plasma density is the critical density. Our results, however, are also valid for the nonresonant case, since they do not depend on the absolute plasma density as long as enough free charge exists to build the grating fringes.

II. FRINGE FORMATION

Let us consider the situation depicted in Fig. 1, where two *s*-polarized laser beams, *I* and *II*, are aimed at a preformed plasma at incidence angles of α and $-\alpha$. The incident beams are represented by harmonic plane waves:

$$\vec{E}_I(\vec{r},t)=E_0\cos(\vec{k}_I\cdot\vec{r}-\omega t+\phi_I)\vec{e}_z\,,$$

$$\vec{E}_{II}(\vec{r},t)=E_0\cos(\vec{k}_{II}\cdot\vec{r}-\omega t+\phi_{II})\vec{e}_z\,, \tag{1}$$

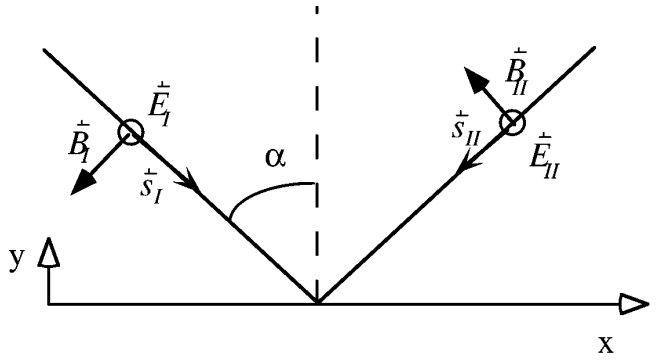

FIG. 1. Scheme of the interaction geometry in the *s*-polarization case. The plasma is approximated by a 1D slab along the *x* direction.

where E_0 is the field amplitude, the same in both beams, and ϕ_I and ϕ_{II} are phase factors. The electric field at the plasma surface ($y=0$) is described by

$$\vec{E}(x,t)=\vec{E}_I(x,t)+\vec{E}_{II}(x,t)=2E_0\cos(\omega t)\cos(kx\ \sin\alpha)\vec{e}_z, \tag{2}$$

where we have moved the coordinate origin so that the phase factors are zero. The magnetic fields associated with the two light beams can be obtained from the electric-field functions by the cross products $\vec{B}_I=\vec{s}_I\times\vec{E}_I$ and $\vec{B}_{II}=\vec{s}_{II}\times\vec{E}_{II}$, where $\vec{s}_I$ and $\vec{s}_{II}$ are the unit vectors along the directions of $\vec{k}_I$ and $\vec{k}_{II}$, respectively. The total magnetic field at the plasma surface is given by

$$B_x(x,t)=-2E_0\cos\alpha\ \cos(\omega t)\cos(kx\ \sin\alpha),$$
$$B_y(x,t)=2E_0\sin\alpha\ \sin(\omega t)\sin(kx\ \sin\alpha). \tag{3}$$

A. Ponderomotive force

For now on we will consider a heavy ion plasma and, therefore, concentrate on the electron dynamics. The electromagnetic force on the electrons is described by the Lorentz equation

$$\vec{F}=q\left(\vec{E}+\frac{\vec{p}}{\gamma m_0 c}\times\vec{B}\right), \tag{4}$$

where p is the particle's momentum, m_0 the rest mass, and

$$\gamma=\left(1+\frac{p^2}{m_0^2c^2}\right)^{1/2}. \tag{5}$$

A first-order approximation for the electron momentum at position x may be calculated neglecting the magnetic-field contribution,

$$p_z(x,t)\simeq q\int_0^t E_z(x,t')dt'=\frac{2qE_0}{\omega}\ \sin\omega t\ \cos(kx\ \sin\alpha), \tag{6}$$

and $p_x(x,t)\simeq p_y(x,t)\simeq 0$. If we insert Eq. (6) into Eq. (4), we have a second-order approximation for the electromagnetic force, valid provided we are not in the ultrarelativistic regime ($v\simeq c$).

The electron dynamics described by Eqs. (6) and (4) leads to a complex electron motion. The electron will quiver mostly in the z direction, with a small drift along the x axis due to the ponderomotive force. If we compute the cycle-averaged force, the quiver term averages to zero, and the motion is governed by the ponderomotive term

$$\langle\vec{F}\rangle=\left\langle\frac{qp_z}{\gamma m_0 c}B_x\right\rangle\vec{e}_y-\left\langle\frac{qp_z}{\gamma m_0 c}B_y\right\rangle\vec{e}_x. \tag{7}$$

Regarding Eqs. (3) and (6), the y component of the ponderomotive force averages to zero; therefore,

$$\langle\vec{F}\rangle=\frac{2q^2}{m_0 c\omega}E_0^2\sin\alpha\ \sin(2kx\ \sin\alpha)\left\langle\frac{\sin^2\omega t}{\gamma(x,t)}\right\rangle\vec{e}_x. \tag{8}$$

A picture of the phenomena enclosed in Eq. (8) can be drawn in the nonrelativistic limit, i.e., $\gamma\simeq 1$. The simple spatial dependence of the ponderomotive force shows that the electrons will be drifted to the equilibrium points at

$$x_m=\frac{2m+1}{4\ \sin\alpha}\lambda, \tag{9}$$

where stability conditions exist. This negative charge accumulation forms fringes along the y direction, giving rise to a diffraction grating structure at the plasma surface. Stability is ensured not only by the sign of the second spatial derivative of the ponderomotive force, but also from the fact that the quiver electron oscillation will be mainly in the z direction, due to the pre-eminence of the electric term in the Lorentz force, provided $v<c$.

B. *P* polarization

A calculation of the same fashion as above may be carried out for the case in which the light beams are p polarized. In this case we have the following expressions by the electromagnetic field components

$$B_z=2E_0\cos\omega t\ \cos(kx\ \sin\alpha),$$
$$E_x=2E_0\cos\alpha\ \cos\omega t\ \cos(kx\ \sin\alpha), \tag{10}$$
$$E_y=-2E_0\sin\alpha\ \sin\omega t\ \sin(kx\ \sin\alpha).$$

Ponderomotive force may be calculated in the same way as before, giving as a result the same situation as for the s-polarization case. Electrons would, therefore, tend to accumulate at the same x_m coordinates, where the ponderomotive potential has a stable minimum. This, however, will not be the case, since the x component of the electric field will induce a quiver perturbation along this axis which will be larger than ponderomotive force, provided we are not in the ultrarelativistic regime.

III. FRINGE DESCRIPTION

It is possible to obtain an analytical approximation for the averaged electron density shown in Figs. 3 and 4. To do this, we first have to compute the time average term of the ponderomotive force given in Eq. (8). Using Eqs. (5) and (6), the cycle time average can be integrated to give

$$\left\langle\frac{\sin^2\omega t}{\gamma(t)}\right\rangle=\left\langle\frac{\sin^2\omega t}{\sqrt{1+K(x)\sin^2\omega t}}\right\rangle=\tfrac{1}{2}F[\tfrac{1}{2},\tfrac{3}{2};2;-K(x)], \tag{11}$$

where $K(x)=[(2qE_0/\omega m_0 c)\cos(kx\sin\alpha)]^2$, and $F(a,b;c;z)={}_2F_1(a,b;c;z)$ is the hypergeometric function. The ponderomotive force is, therefore,

$$\langle\vec{F}\rangle=\frac{q^2\sin\alpha}{m_0 c\omega}E_0^2\sin(2kx\sin\alpha)F[\tfrac{1}{2},\tfrac{3}{2};2;-K(x)]\vec{e}_x. \tag{12}$$

Let us now study a neighbor region of the plasma surface around the stability point x_m of width $2x$. Let $Q(x)$ be the time-averaged amount of charge enclosed in such region.

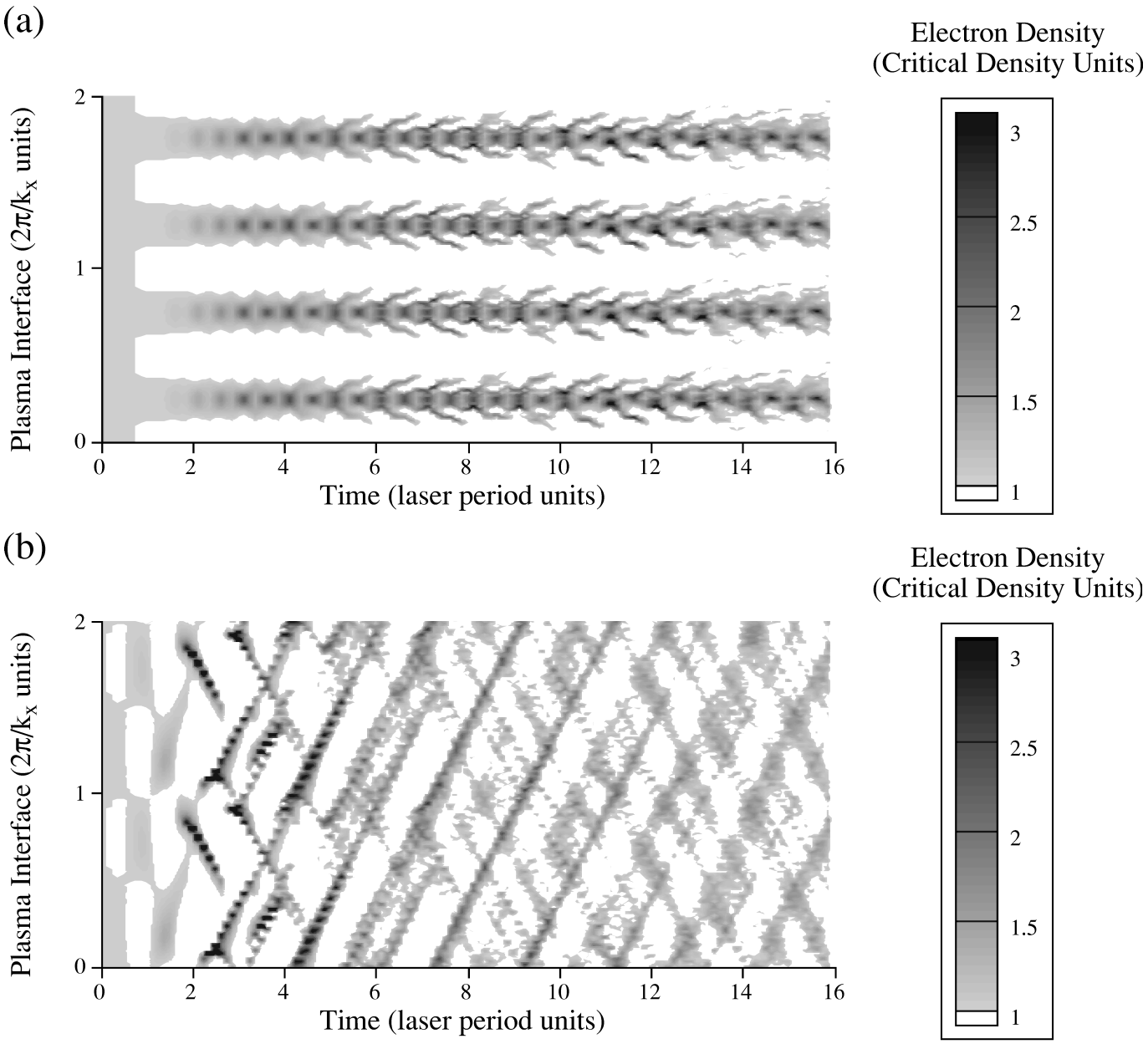

FIG. 2. Time evolution of the electron density as calculated from the PIC code, for *s* polarization (a) and *p* polarization (b). The interaction time is plotted along the horizontal axis and a space region of twice the wavelength of the projected wave number on the *x* coordinate is plotted along the vertical axis. The beam intensity is 10^{18} W/cm^2, wavelength 0.8 μm, and the angle of incidence $\alpha=\pi/3$ rad. The plasma density is initially equal to the critical density $n_c=1.76\times10^{21}$ cm^{-3}. To enhance fringe visibility, the electron density above critical is plotted on a scale of grey tones, while densities below critical are plotted in white. The formation of fringes in the *s*-polarization set up becomes apparent before the four-cycle turn-on is completed. No grating structure is present in the *p*-polarization case.

The electrostatic field at the edge of the region x_m+x can be calculated through Gauss' theorem to be $E_{st}=4\pi Q$. For a stable situation to occur, the electrostatic force must be compensated for by the ponderomotive, therefore $qE_{st}(x_m+x)+\langle F\rangle(x_m+x)=0$. Therefore the enclosed charge will be

$$Q(x)=\frac{q\ \sin\alpha}{4\pi m_0 c\omega}E_0^2\sin(kx\sin\alpha)F[\tfrac{1}{2},\tfrac{3}{2};2;-K(x)]. \tag{13}$$

The electron charge density may be found as the spatial derivative of the enclosed charge $Q(x)$ plus the unperturbed charge density, ρ_0. The final expression reads

$$\rho(x)=\frac{1}{2\pi}\frac{q}{m_0c^2}E_0^2\sin^2\alpha\ \cos(2kx\sin\alpha)F[\tfrac{1}{2},\tfrac{3}{2};2;-K(x)] + \frac{3}{8\pi}\frac{q}{m_0c^2}\left(\frac{qE_0}{m_0c\omega}\right)^2E_0^2\sin^2\alpha \times\sin^2(2kx\ \sin\alpha)F[\tfrac{3}{2},\tfrac{5}{2};3;-K(x)]+\rho_0 \tag{14}$$

IV. PIC SIMULATIONS

To test the preceding ideas, we performed particle-in-cell calculations (1D3V PIC) [8], one dimensional (1D) in real

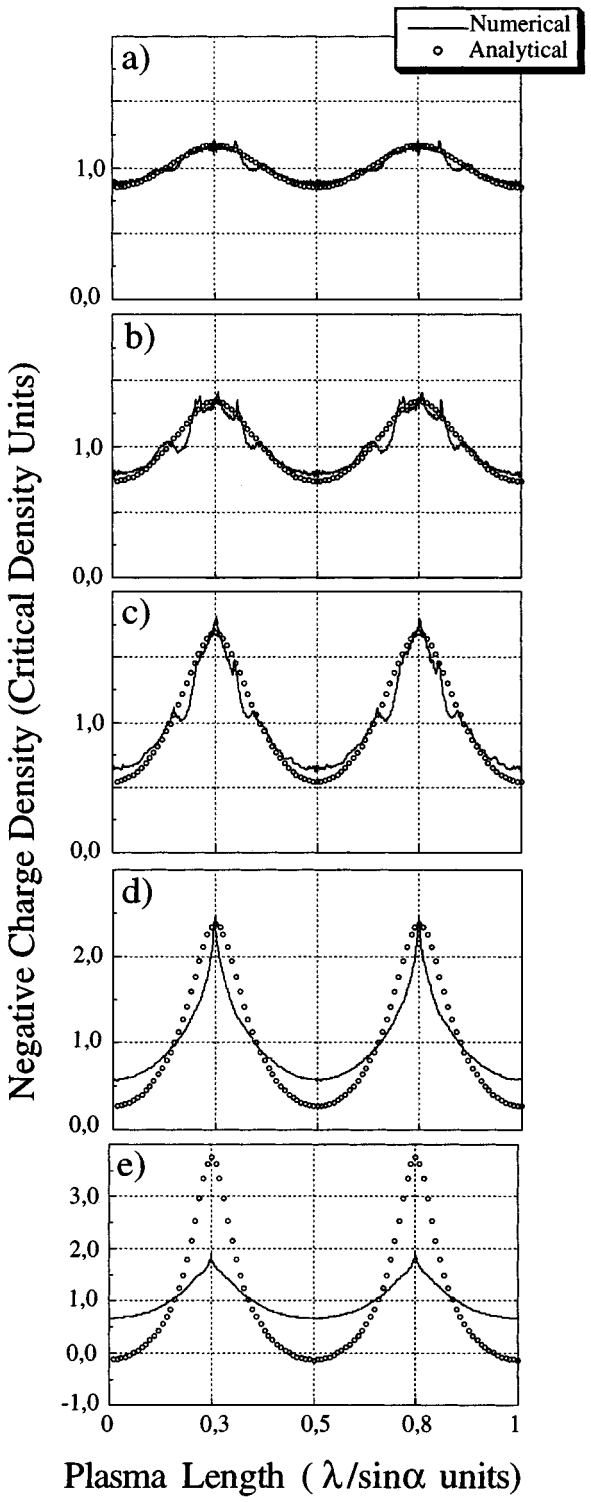

FIG. 3. Time-averaged electron density as a function of the spatial coordinate. The solid line shows the result of the PIC simulations while circles show the analytical prediction. All parameters are the same as in Fig. 2, except for the field intensity: (a) 2.5 $\times 10^{17}$, (b) 5×10^{17}, (c) 10^{18}, (d) 2×10^{18} and (e) 4×10^{18} W/cm^2.

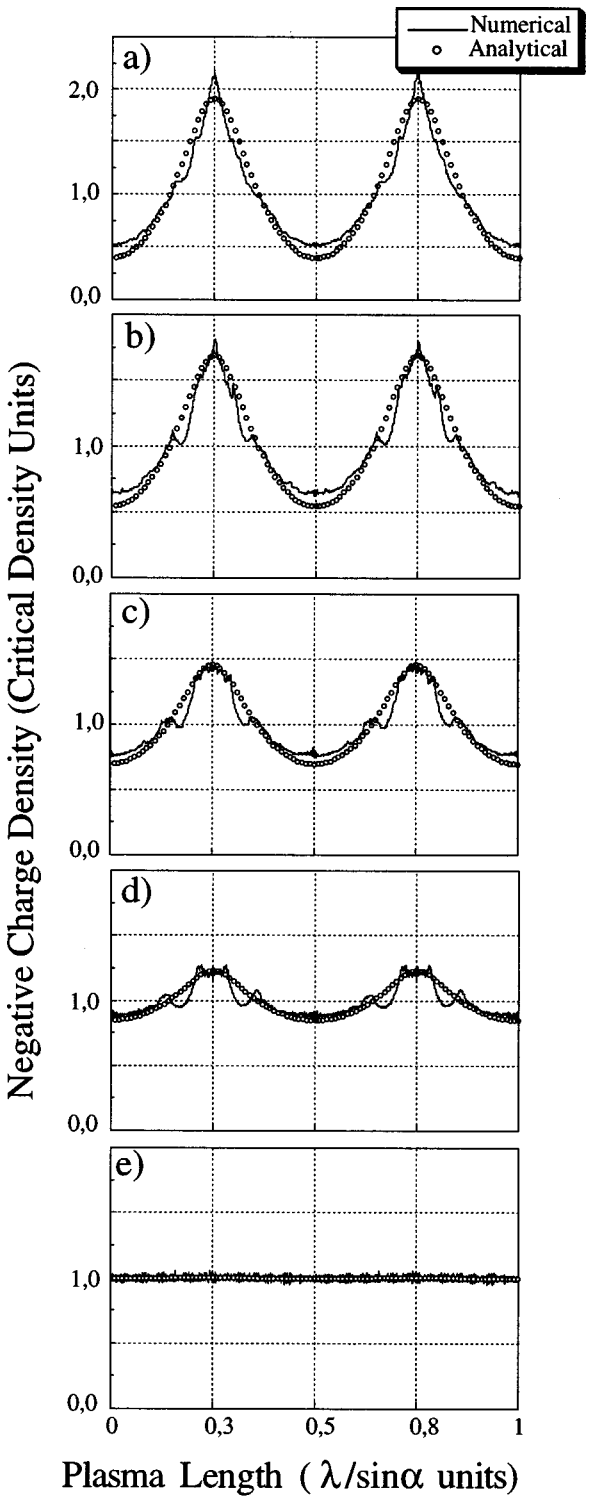

FIG. 4. Time-averaged electron density as a function of the spatial coordinate. The solid line shows the result of the PIC simulations while circles show the analytical prediction. All parameters are the same as in Fig. 2, except for the angle of incidence: (a) 85.7°, (b) 60°,(c) 45°,(d) 30°, and (e) 4.5°.

space and three dimensional in velocity space, for different incident angles, field intensities, and polarizations. Electron charges are represented by quasiparticles in a one-dimensional space along the x coordinate, and in three-dimensional velocity space. In the s-polarization regime, the electron density will be approximately invariant to a translation in the z coordinate if $v<c$. Also, the quiver along the y axis will be small, since it will be driven only by magnetic force terms. In addition, for particles detached from the surface, the drift motion along the y coordinate will be reduced, if not suppressed, by the restoring force coming from the

Coulomb interaction between the detached charges and the depleted surface. The 1D approach is, therefore, justified. In the p-polarization case, the x and y terms of the electric field will promote strong quiver in the y direction. The plasma restoring force may not be strong enough to avoid surface ionization. In this case, the 1D approximation is, certainly, less convincing. This regime, however, was shown to be unstable in Sec. III, and, therefore, of less interest to our purposes.

Our PIC code solves the Poisson equation in the reciprocal space, and the Lorentz equation for each particle. Since our plasma slab is assumed to have thickness 0, the field acting on the charges is well approximated by the incident field, i.e., neglecting the effect of propagation through the plasma medium. This, together with the fact that we are not interested in the study of the reflected and transmitted field in this paper, makes unnecessary the integration of the other three Maxwell equations.

The electromagnetic fields are described by plane-wave expressions, with time-dependent envelope consisting of four turn-on cycles followed by 12 of constant amplitude E_0. The turn-on term $\sin^2(\pi t/T_{\rm on})$ induces our system adiabatically into a quasistationary regime.

Figure 2(a) shows the negative charge density along a region of width $2\pi/k_x$ in the x direction, as a function of time. The s-polarized laser pulses have a turn-on of four cycles followed by 12 cycles of constant amplitude, and are aimed at incident angles (α) of $\pi/3$ and $-\pi/3$ respectively. The plasma is assumed to be preformed before the pulse interaction, and has a density equal to the critical (1.76×10^{21} cm^{-3}). The electric-field amplitude is 5.28 a.u. (intensity of 10^{18} W/cm^2), and the frequency is 0.057 a.u. ($\lambda=0.8$ μm). Fringes are formed after a few cycles, and retain their relevant characteristic over the whole calculation. Figure 2(b) shows the same calculation for a p-polarization arrangement. In agreement with the discussion above, stability conditions are not achieved, and no fringe structure is present.

A more compact visualization of these results is shown in Fig. 3, where the negative charge density, averaged over the total calculation time, is plotted for different field amplitudes (solid line) compared to the result of the analytical expression, Eq. [14] (circles). The analytical expression for the average charge density shows a good agreement with the PIC simulation results for intensities below 2×10^{18} W/cm^2. As the electric-field amplitude increases, the fringes become more pronounced and their width shrinks [Figs. 3(a)–3(d)]. For very intense fields, however, the amount of charge stored in the fringes diminishes [Fig. 3(e)]. This can be explained by the increase of the quiver oscillation amplitude induced by the magnetic terms, when we approach the ultrarelativistic regime. For this regime, the analytical expression overestimates the numerical results.

In Fig. 4 we plot the averaged charge density as the angle of incidence diminishes. The maximum electron density decreases as the angle decreases and we approach the normal incidence. The fringe width increases approximately at a rate $1/\sin\alpha$.

V. CONCLUSIONS

We have discussed the possibility of inducing a grating structure in the surface of a plasma, through the interaction with two high-intensity crossed laser beams. A simple weak relativistic model can be drawn for the time-average dynamics that shows a stable situation when the beams are s polarized. Also with this model we can give an approximate analytical expression for the time-averaged charge density, showing the fringe modulations. The results from our model are compared with the direct integration of the Lorentz and Poisson equations by means of a one-dimensional particle-in-cell code. This shows that the derived expression for the charge density is a reasonable description as long as we do not enter into the ultrarelativistic regime.

ACKNOWLEDGMENTS

We acknowledge discussions with Isabel Arias, Andrea Macchi, and P. Audebert. Partial support from the Spanish Dirección General de Investigación Científica y Técnica (Grant No. PB95-0955), from the Junta de Castilla y León (Grant No. SA81/96), and from the European Comission Training and Mobility of Researchers Program (under Contract No. ERBFMRXCT96-0080) is acknowledged.

[1] An overview of these phenomena can be found in *Atoms in Intense Laser Fields*, edited by M. Gavrila, Advances in Atomic, Molecular and Optical Physics (Academic, Boston, 1992).

[2] L. Plaja and L. Roso, Phys. Rev. B **45**, 8334 (1992).

[3] A review on the relevant aspects of short pulse laser-plasma interaction can be found in P. Gibbon and E. Förster, Plasma Phys. Controlled Fusion **38**, 769 (1996).

[4] G. Farkas, C. Toth, S. D. Moustaizis, N. A. Papadogiannis, and C. Fotakis, Phys. Rev. A **46**, R3605 (1992).

[5] D. von der Linde, T. Engers, G. Jenke, P. Agostini, G. Grillon, E. Nibbering, A. Mysyrowicz, and A. Antonetti, Phys. Rev. A **52**, R25 (1995).

[6] R. Lichters, J. Meyer-ter-Vehn, and A. Pukhov, Phys. Plasmas **3**, 3425 (1996).

[7] P. Gibbon, Phys. Rev. Lett. **76**, 50 (1996).

[8] C. K. Birdsall and A. B. Langdon, *Plasma Physics via Computer Simulation*, Plasma Physics Series (Institute of Physics, Bristol, 1991).

[9] D. von der Linde and K. Rzążewski, Appl. Phys. B **63**, 499 (1996).

[10] S. V. Bulanov, N. M. Naumova, and F. Pegoraro, Phys. Plasmas **1**, 745 (1994).

[11] H. Kalt, V. G. Lyssenko, R. Renner, and C. Klingshirn, J. Opt. Soc. Am. B **7**, 1188 (1985), and references therein.

[12] V. V. Elisseev, W. Rozmus, V. T. Tikhonchuk, and C. E. Capjack, Phys. Plasmas **3**, 2215 (1996).